
Article:
Blitz, MA orcid.org/0000-0001-6710-4021, Salter, RJ, Heard, DE orcid.org/0000-0002-0357-6238 et al. (1 more author) (2017) An Experimental and Master Equation Study of the Kinetics of OH/D + SO_2: The Limiting High Pressure Rate Coefficients. Journal of Physical Chemistry A, 121 (17). pp. 3184-3191. ISSN 1089-5639

https://doi.org/10.1021/acs.jpca.7b01295

An Experimental and Master Equation Study of the Kinetics of OH/OD + SO_2: the Limiting High Pressure Rate Coefficients

Mark A. Blitz,[a,b]* Robert J. Salter,[a,c] Dwayne E. Heard [a,b] and Paul W. Seakins [a,b]

[a] School of Chemistry, University of Leeds, Leeds, LS2 9JT, UK

[b] National Centre for Atmospheric Science, University of Leeds, Leeds, LS2 9JT, UK

[c] Now at Deloitee MCS, 3 Rivergate, Temple Quay, Bristol, BR1 6GD, UK

*E-mail: m.blitz@leeds.ac.uk

Abstract

The kinetics of the reaction OH/OD + SO_2 have been studied using a laser flash photolysis / laser induced fluorescence technique. Evidence for two-photon photolysis of SO_2 at 248 nm is presented and quantified, and which appears to have been evident to some extent in most previous photolysis studies, potentially leading to values for the rate coefficient, k_1, that are too large. The kinetics of the reaction OH(v=0) + SO_2 (T = 295 K, p = 25 – 300 Torr) were measured under conditions where SO_2 photolysis was taken into account. These results, together with literature data, were modelled using a master equation analysis. This analysis highlighted problems with the literature data: the rate coefficients derived from flash photolysis data were generally too high and from the flow tube data too low. Our best estimate of the high-pressure limiting rate coefficient, k_1^∞, was obtained from selected data and gives a value of $(7.8 \pm 2.2) \times 10^{-13}$ cm^3 $molecule^{-1}$ s^{-1}, which is lower than that recommended in the literature. A parameterized form of $k_1([N_2],T)$ is provided. The OD(v=0) + SO_2 (T = 295 K, p = 25 – 300 Torr) data are reported for the first time and master equation analysis reinforces our assignment of k_1^∞.

1. Introduction

.

In our companion paper the limiting high-pressure rate coefficient, k_1^∞ for the reaction:

$$OH + SO_2 (+ M) \rightarrow HOSO_2 (+ M) \qquad R1$$

was investigated by measuring the removal rate coefficient of vibrationally excited OH/OD in the presence of SO_2 as a function of temperature. This study revealed that the removal rate coefficient increased with vibrational level, which implies that the OH/OD(v = 1) + SO_2 removal rate coefficient, previously used as an estimate of the high pressure limit, k_1^∞,[1] via the proxy method,[2] is an overestimation. Further analysis of these data was able to identify k_1^∞, albeit with significant error, $(7.2 \pm 3.3) \times 10^{-13}$ cm^3 $molecule^{-1}$ s^{-1}. This value for k_1^∞ is smaller than the recommended literature values from IUPAC and JPL, $(2.0^{+2.0}_{-1.0})$ and $(1.6 \pm 0.4) \times 10^{-12}$ cm^3 $molecule^{-1}$ s^{-1}, respectively.[3-4] In this paper we report data on k_1 as a function of pressure, coupled with an extrapolation to the high pressure limit using a master equation analysis, which reinforces our lower value for k_1^∞ and highlights the problems in the literature data.

Reaction R1 is pressure dependent and is in its falloff regime at atmospheric pressure and below. The kinetics of R1 in this pressure regime have been extensively studied,[5-8] and Rice-Ramsperger-Kassel-Markus (RRKM) modelling of these data has been used to recommend the limiting high-pressure rate coefficient: Wine et al. recommended a value for k_1^∞ between 260 and 420 K equal to 1.3×10^{-12} $(T/300\ K)^{-0.7}$ cm^3 $molecule^{-1}$ s^{-1} and Cobos and Troe [9] recommended $k_1^\infty = 2.7 \times 10^{-12}$ $exp(-80K/T)$ cm^3 $molecule^{-1}$ s^{-1} ($k_1^\infty(300\ K) = 2.1 \times 10^{-12}$ cm^3 $molecule^{-1}$ s^{-1}). More recently Fulle et al. [10] measured k_1 over an extended pressure range up to 96 bar and their estimate of k_1^∞ was significantly larger than the above recommendations, and a significant positive

activation energy was observed, contrary to the recommendations. The evaluations by IUPAC [3] and JPL [4] recommended the values: k_1^∞(250–300 K) = 2.0 and 1.6 × 10^{-12} cm^3 $molecule^{-1}$ s^{-1} and k_1(1 bar N_2, 298 K) = 8.9 and 9.5 × 10^{-13} cm^3 $molecule^{-1}$ s^{-1}, respectively.

In this study the two-photon 248 nm photolysis of SO_2 is quantified, and it is suggested that previous studies have overestimated k_1^∞ as details of this effect (single or two-photon photolysis) were not taken into account. OH(v =0) + SO_2 rate coefficients were determined under conditions that took two-photon SO_2 photolysis into account, and then master equation analysis (using the Master Equation Solver for Multi Energy-well Reactions (MESMER) code [11]) was used to fit these data and selected literature data in order to determine k_1^∞. OD(v =0) + SO_2 rate coefficients were also determined and these represent the first such measurements, but no MESMER analysis has been performed with this data. Both the current and the companion paper returned a consistent value for k_1^∞, which is significantly lower than the currently recommended value.

2. Experimental

Photolysis / Laser Induced Fluorescence

The experimental methods are similar to those described previously,[1,12] thus only the salient features are highlighted. The apparatus used to perform the OH/OD(v = 0) + SO_2 study was similar to that used in the vibrationally excited state OH/OD(v = 1,2,3) kinetics study in the companion paper. An excimer laser (Lambda Physik, LPX 210) was used as the photolysis laser, with the pulse energy controlled using a combination of the high voltage power supply and metal gauze attenuation filters. An energy meter

(JMAX11, Molectron) was used to measure the output of the excimer laser. The ground state hydroxyl (OH/OD) radical was monitored by on-resonant laser induced fluorescence (LIF) at ~ 308 nm using the doubled output from an excimer laser (Lambda Physik, LPX 100) pumped dye laser (Lambda Physik, FL2002), which operated with the dye Rhodamine B. The subsequent fluorescence ($A^2\Sigma^+ \rightarrow X\ ^2\Pi_i$) was passed through a 308 nm interference filter and was detected using a photomultiplier (Electron Tubes 9813); the resultant signal was integrated and digitized on a LeCroy (Waverunner LT372) oscilloscope before being transferred for storage on a PC. Over the region 280-290 nm, the laser excitation wavelength conventionally used for off-resonant OH detection, fluorescence from other species was detected. Hence, ground-state OH/OD was detected resonantly at 308 nm; although there was significant scattered probe laser light, it did not significantly affect the later time hydroxyl fluorescence signal. A LabVIEW program controlled the delay generator which scanned the time delay between the photolysis and probe laser, and recorded the OH/OD signal via the oscilloscope. Typically, the time delays were scanned over 200 - 400 points, with each point being the average of up to ten samples. The lasers were fired at a pulse repetition frequency of 5 Hz.

The gases were introduced into the reaction cell through a mixing manifold. Control of the gas flow was regulated by calibrated mass flow controllers. After the mixing manifold, the gases entered a ten-way cross stainless steel reaction cell. The pressure in the cell was regulated by throttling the exit valve of the cell and monitored via a capacitance manometer. The total flow was greater than 10 sccm per Torr total pressure, ensuring that the gases were swept through the cell between laser pulses.

SO_2 and $(CH_3)_3COOH$ (Sigma Aldrich, 99.9% and 70%, respectively) were purified by first degassing and then diluted in He. H_2 / D_2 (Air Products, 99.999%) and He (BOC, CP grade 99.999%) were used directly from the cylinder.

Master Equation Analysis

Master equation calculations have been carried out using the program MESMER (Master Equation Solver for Multi Energy-well Reactions),[11] where the required input parameters for the stationary points were obtained from a recent high level ab initio calculation on $HOSO_2$.[13] The application of the master equation to reactions in the gas phase has been extensively discussed elsewhere.[11, 14-17] Here, the main points are summarized and the manipulations required to accommodate second order systems are discussed.

The system is set up by dividing the energy of $HOSO_2$ into grains, and the time evolution of the system is then obtained by solving the energy grained master equation:

$$\frac{d}{dt}\mathbf{p} = \mathbf{Mp} \qquad \text{(E1)}$$

where **p** is the population vector containing the population, n(E), of energy grains from $HOSO_2$ and **M** is the matrix that describes collisional energy transfer between grains and reaction from grains, and also includes a bimolecular source term in order to describe formation of $HOSO_2$ via bimolecular reaction. Eqn (E1) represents a set of coupled differential equations and was solved to yield:

$$\mathbf{p} = \mathbf{U}e^{\lambda t}\mathbf{U}^{-1}\mathbf{p}(0) \qquad \text{(E2)}$$

where $\mathbf{p}(0)$ contains the initial conditions for each grain, $\mathbf{U}$ is an eigenvector matrix obtained from the diagonalization of $\mathbf{M}$, and λ is the diagonal matrix of corresponding eigenvalues, where the smallest eigenvalues are the chemically significant eigenvalues. Time-dependent concentrations of different species were obtained by summing the normalized populations from Eqn (E2) over the appropriate grains. The phenomenological rate coefficients were extracted from the chemically significant eigenvalues.[11]

In the MESMER calculation for the OH + SO_2 association reaction, the microcanonical rate coefficients for dissociation of the $HOSO_2$ adduct, k(E), have been calculated using the pragmatic approach of taking the Inverse Laplace Transform (ILT) of the pressure limiting rate coefficient, $k_1^{\infty}(T)$. This has an exact solution when $k^{\infty}(T)$ can be represented by the form:[18]

$$k^{\infty}(T) = A\left(\frac{T}{T_0}\right)^n \exp(-E_a / RT) \qquad \text{(E3)}$$

In the present work, T_0 was set to 298 K and E_a set to 0 kJ mol^{-1}, so the temperature dependence is wholly controlled via n. A value of n equal to 0.1 was determined over the temperature range 295 – 800 K in the companion paper. This approach has the advantage that the parameters defining the high pressure limiting rate coefficient, a principal target of the present two papers, are determined directly from the MESMER fit to the experimental data. The vibrational and rotational constants together with the $HOSO_2$ adduct zero point energy were fixed to the literature,[13] and systematic Lennard-Jones parameters were chosen. In the SI the input parameters for this MESMER calculation are given.

The rates of reaction from OH + SO_2 into a particular grain of $HOSO_2$ were determined by detailed balance.[19] An exponential down model, coupled with detailed balance, was used for the probabilities of collisional energy transfer between the grains, based on the parameterization $\langle\Delta E\rangle_{down} = \langle\Delta E\rangle_{down,298}(T/298\ K)^m$, where $\langle\Delta E\rangle_{down}$ is the average transferred in a downward direction.[20] All of the available data were fitted to the master equation model, using the minimization of χ^2:

$$\chi^2 = \sum_{i=1}^{N} (k_{i,exp} - k_{i,model})^2 / \sigma_i^2 \qquad \text{(E4)}$$

as the criterion of best fit. Here $k_{i,exp}$ is the ith experimental rate coefficient, $k_{i,model}$ is the model result under the same conditions of T and p, σ_i is the standard deviation of the experimental rate coefficient and N is the total number of experimental measurements. The analysis was conducted, as were the experiments, under pseudo first order conditions ([OH] << [SO_2]). The bimolecular forward rate coefficient, k_{bim} was used in the fits and [SO_2] was given a fixed value of 10^{15} molecule cm^{-3}. The variable parameters in the fitting process were A, n, $\langle\Delta E\rangle_{down,298}$. The best available experimental data (literature values and the values determined here) were all simultaneously used in a global fit.

3. Results

SO_2 + 2hv $\rightarrow$ $O(^1D)$ + SO

The two photon dissociation of SO_2 (P1) involves initial promotion of the $SO_2(X)$ ground state to the long-lived B-state (τ=10-100 μs); the second photon further excites

SO_2 from this B-state to a dissociative state, which rapidly leads to products. Effenhauser et al.[21] studied this process at 248 nm using photofragment translational spectroscopy and observed 9 distinct processes:

$$SO_2 + 2\,h\nu_{248\,nm} \rightarrow SO\,(X^3\Sigma^-), (a^1\Delta), (b^1\Sigma^+) + O\,(^1D), (^3P) \qquad (P1a)$$

$$\rightarrow O_2\,(X^3\Sigma^-_g) + S\,(^3P) \qquad (P1b)$$

$$\rightarrow O_2\,(X^3\Sigma^-_g) + S\,(^1D) \qquad (P1c)$$

$$\rightarrow O_2\,(a^1\Delta_g) + S\,(^1D) \qquad (P1d)$$

but were unable to quantify the contributions from each channel.

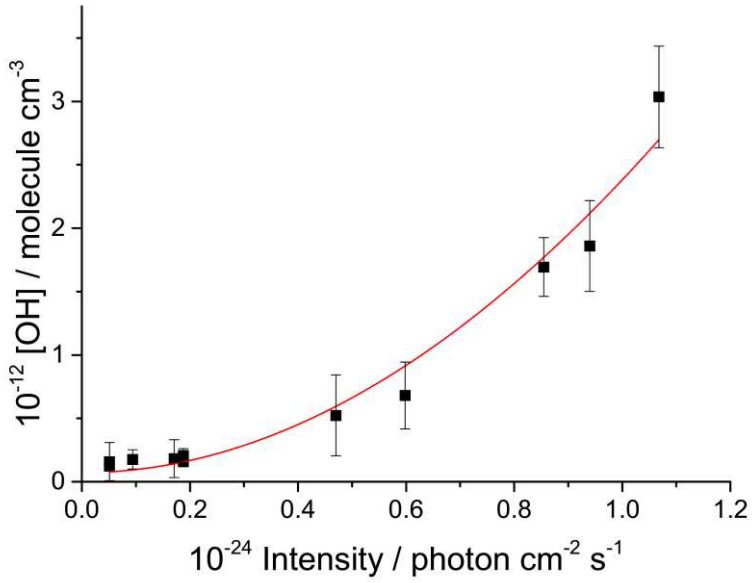

Figure 1. OH production from P1 and R2 as a function of excimer laser intensity. The duration of the excimer laser pulse was 20 ns. The red line is a quadratic function fitted to the data.

The cross-section for P1a to produce $O(^1D)$ was determined by measuring the OH signal as a function of laser energy:

$$O(^1D) + H_2 \rightarrow OH\,(v = 0\text{–}4) + H \qquad (R2)$$

where $[H_2] >> [SO_2]$ to ensure $O(^1D)$ is converted to OH, i.e $[O(^1D)]_0 = [OH]$.[22] OH(v =1,2,3) in the presence of SO_2 rapidly cascade down to OH(v = 0), which is slowly lost

primarily via reaction with SO_2 at ~25 Torr total pressure. Hence, the total amount of OH in the system is readily determined from the OH(v = 0) time trace. Figure 1 shows that the [OH] concentration increases with a quadratic dependence on laser fluence, consistent with a two photon process. In our previous paper on two photon dissociation of benzene,[23] we showed this quadratic dependence can be used to assign the second photon absorption cross-section, if the first photon absorption cross-section and the absolute radical concentration are known. The first absorption cross-section in SO_2 at 248 nm, σ_1, is 6×10^{-20} cm^2 $molecule^{-1}$ [24] and allows the concentration of excited state SO_2, SO_2*, to be calculated:

$$[SO_2^*]_0 = [SO_2]_0 \, \sigma_1 \, F \qquad \text{(E5)}$$

where F is the laser fluence. The second photon absorption from the SO_2* state leads to OH via, P1a and R2, with a concentration given by:

$$[OH]_0 = [SO_2^*]_0 \, \sigma_2 \, F \qquad \text{(E6)}$$

where σ_2 is the second photon absorption cross-section leading to the formation of $O(^1D)$, P1a. Equations 5 and 6 lead to the OH concentration given by:

$$[OH]_0 = [SO_2]_0 \, \sigma_1 \, \sigma_2 \, F^2 \qquad \text{(E7)}$$

The OH concentration (= $[O(^1D)]$) can be assigned by comparison to a known OH precursor. In the present study the absolute OH concentration was assigned by comparison to the OH signal from 248 nm photolysis of known concentrations of t-$(CH_3)_3COOH$:[25]

$$\text{t-}(CH_3)_3COOH + h\nu_{248\,nm} \rightarrow OH(v=0) + \text{co-products} \qquad \text{(P2)}$$

Fitting equation E7 to the data in Figure 1 gives $\sigma_2 = (5.5 \pm 2.0) \times 10^{-18}$ cm^2 $molecule^{-1}$. This cross-section is smaller than the total absorption cross-section as it is only for the channel that produces $O(^1D)$. As $\sigma_2 > \sigma_1$, absorption of the second photon occurs much

more readily than the first, and consequently a significant fraction of SO_2 absorption results in photodissociation. In fact, probing OH(v = 0) at 282 nm was not possible as the OH fluorescence signal was overwhelmed by signal from other species, presumably from SO. In addition, a small signal, ~ 100 μs lifetime, was observed from photolysis of SO_2 alone and was assigned to emission from excited SO. This background signal was accounted for by recording a kinetic trace without the probe.

OH/OD(v=0) + SO_2

Some OH (v =0) + SO_2 experiments were carried out using the precursor t-$(CH_3)_3COOH$.[25] The OH from this precursor was observed to depend linearly on laser photolysis energy, and via its 248 nm absorption cross-section, was used to calibrate the OH concentration in the SO_2 two photon photolysis experiments. To counteract the problem of reaction between OH and photoproducts from SO_2 photolysis while studying OH(v=0) + SO_2, it was arranged that the photolysis laser energy was adjusted, via wire mesh attenuators, so that the amount of SO_2 photolysis products were constant as the SO_2 concentration was varied. Hence, the reaction between OH and photoproducts was present in the intercept of the bimolecular plots and not in the slope.

A few OH(v=0) experiments and all the OD (v=0) were carried out using the same methods used to generate the vibrationally excited state, i.e. photolysis of $SO_2/H_2/D_2$, where the photolysis energy was again suitably adjusted to ensure that the photolysis products were constant as the SO_2 concentration was varied. It is acknowledged that this photolysis laser adjustment, see Figure 1, was only crudely achieved by mesh filters. It is estimated the contribution from OH + SO_2 photo-products was kept constant to within 30 %.

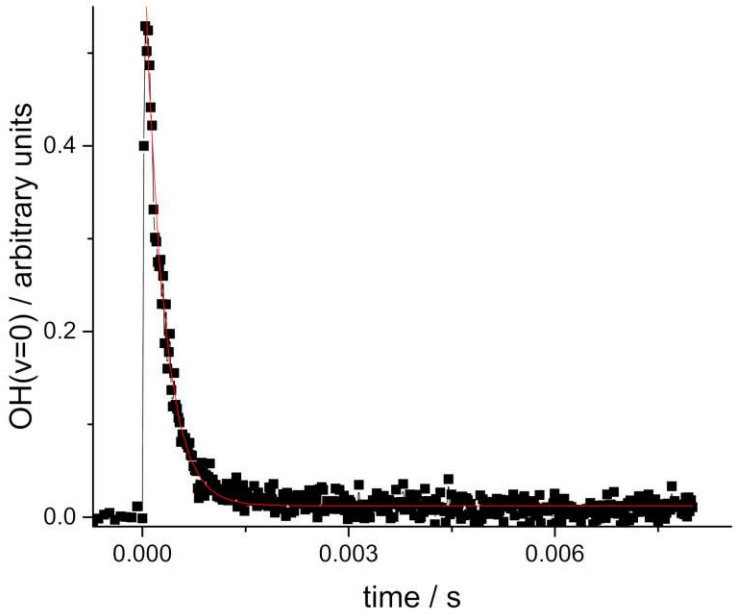

Figure 2. OH(v=0) + SO_2 (2.35×10^{16} molecule cm^{-3}) at 50 Torr total pressure, helium. t-$(CH_3)_3COOH$ was used to generate ground-state hydroxyl radical. Analysis of these data (E8) yields k_{obs} = (3643 ± 63) s^{-1}, where the error is statistical at the 1 σ level. The red line is the best fit to the data.

The pressure and temperature dependence of the reaction OH/OD(v=0) + SO_2 was studied via experiments using helium buffer gas. Photolysis of t-$(CH_3)_3COOH$ only produced OH in its ground vibrational state, so that the decay of [OH(v=0)] in the presence of SO_2 was observed to obey single exponential behaviour (see Figure 2):

$$[OH(v=0)] = [OH(v=0)]_0 \exp(-k_{obs}t) + B \qquad \text{(E8)}$$

where k_{obs} is the pseudo-first-order rate coefficient and is equal to $k_1[SO_2] + k'_{other}$; k'_{other} should be reasonably constant for all experiments as the photolysis energy was suitably adjusted to ensure that the amount of SO_2 photolysis products were constant. B is a

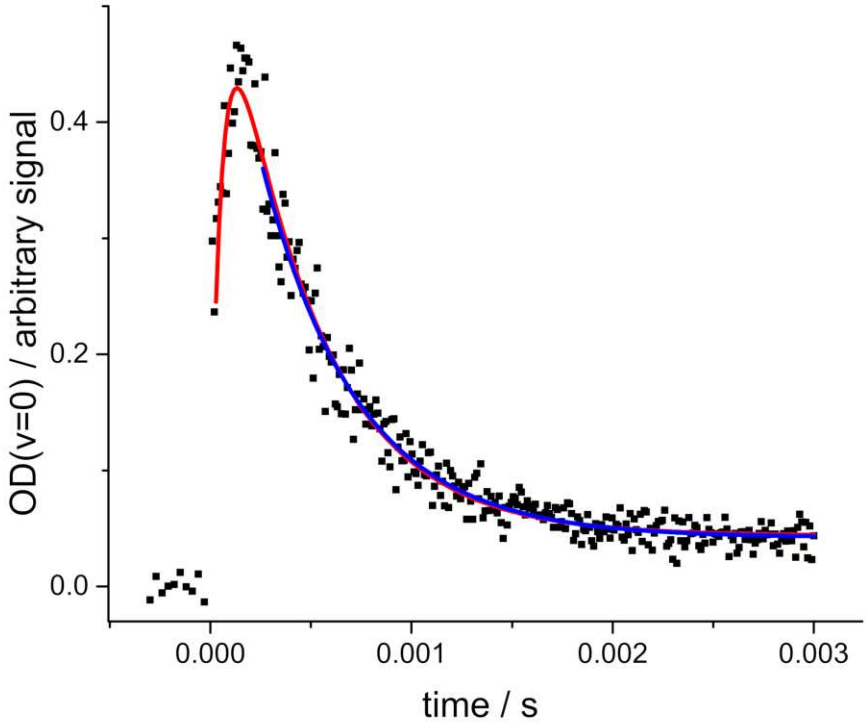

Figure 3. OD(v=0) from the photolysis of SO_2 (6.05×10^{15} cm^{-3}) / D_2 at a total pressure of 100 Torr, helium buffer. At early times there is growth due to relaxation from higher vibrational states, OD(v >0). Soon after the maximum in the OD signal the decay is described by a single exponential (blue curve), which via Eqn (E8) gives k_{obs} = (2107 ± 60) s^{-1}. The red line is a biexponential fit to the data and gives k_{obs} = (2232 ± 69) s^{-1}.

parameter that accounts for the small amount of background fluorescence from non-OH species, see Figure 2. The reaction OD(v=0) + SO_2 was studied using the photolysis of SO_2/D_2 as the radical source. While this method produced vibrationally excited OD radicals, the analysis of OD(v=0) data was straightforward as the vibrationally excited radicals relax much faster than OD(v=0) is removed, see companion paper. This can be seen in Figure 3, where, after only a short time, relaxation is complete and then the data are described by a single exponential, (E8), yielding k_{obs}. In Figure 3, a biexponential fit is also shown – see companion paper for this equation and how it accounts for vibrational relaxation – in order to show that soon after the maximum in the OD signal

the biexponential and exponential fits converge. A few experiments on OH(v=0) were also carried out using photolysis of SO_2/H_2 as the radical source, and produced similar results to using t-butylhydroperoxide photolysis. Plots of k_{obs} versus $[SO_2]$ were fitted to a straight-line where the slope is equal to the bimolecular rate coefficient, k_1. An example of such a plot is given in Figure 4. The bimolecular rate coefficients were then determined over a range of pressures: 25 - 400 Torr and 295 K, see Figure 5. All the results are summarized in Tables 1 (OH) and 2 (OD).

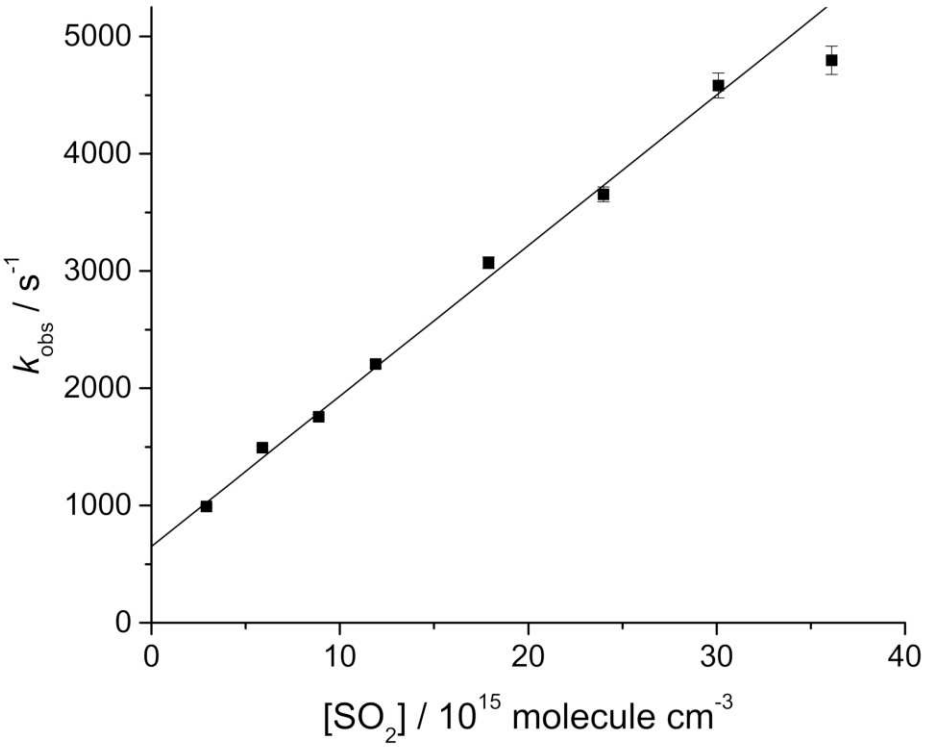

Figure 4 Bimolecular plot of k_{obs} vs $[SO_2]$ for OH(v=0) + SO_2 at 50 Torr total pressure, helium buffer; $k_1 = (1.28 \pm 0.03) \times 10^{-13}$ cm^3 $molecule^{-1}$ s^{-1}.

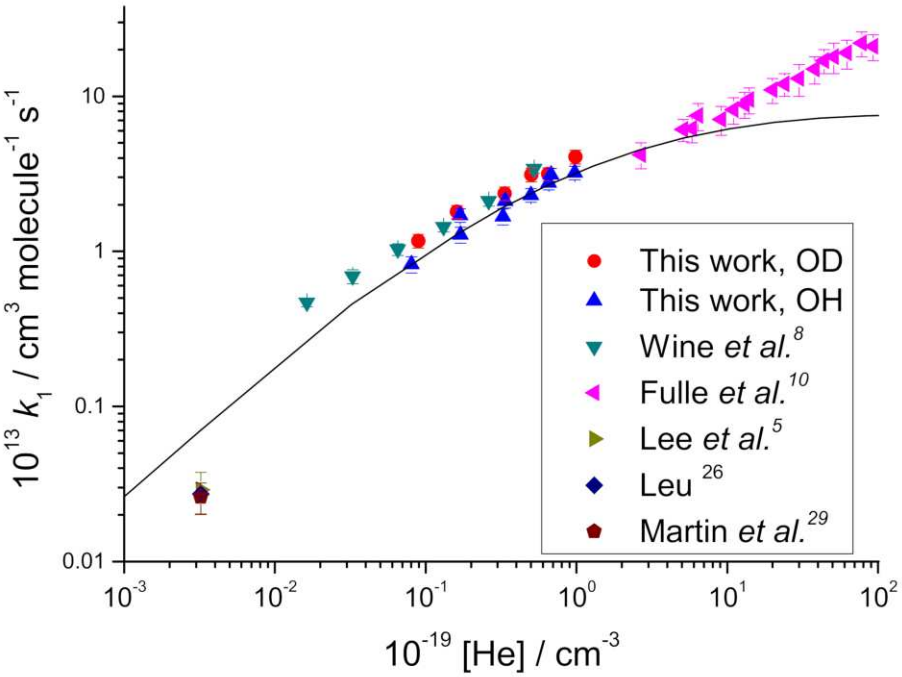

Figure 5. Literature rate coefficients, k_1, for the reaction OH + SO_2, at room temperature, where helium is the bath gas. Our results for OD + SO_2 are also included. The solid line is a master equation simulation for OH + SO_2 using helium and the parameters from the fit to the k_1[M] data in Figure 7, the most reliable data set, see text for details.

In general our values for k_1 are within a factor of ~2 of Wine et al.[8], but as can be seen from Figure 5 (note that this is log-log plot), the low pressure flow tube data from Lee et al., Leu and Martin et al.[5-6, 26] are in serious disagreement based on extrapolation from the high-pressure flash photolysis data. It is noted that all the low-pressure flow tube data are in good internal agreement. [5, 26-29] This discrepancy between the low and high pressure results is further discussed below when full master equation calculations are applied to the data to determine the best estimate for k_1^{∞}(T). Also from Figure 5, it can be seen that the rate coefficients from Fulle et al.[10] increase almost linearly all the way up to 96 bar and from these data a value $k_1^{\infty} = 3.6 \times 10^{-12}$ cm^3

molecule^{-1} s^{-1} was assigned. This result is wholly incompatible with the master equation analysis - see below - where a much lower k_1^{∞} is determined from the experimental data. It is possible that Fulle et al. had not considered SO_2 photolysis - see above - and hence did not account for additional OH removal by radical-radical reactions and therefore overestimated k_1.

5. Discussion

Interpretation of the results for OH(v=0) via master equation analysis

As discussed in the introduction, there is an inconsistency in the experimental values for k_1 for OH(v=0) + SO_2 as a function of pressure and temperature, which means there is a substantial uncertainty in the value of k_1 used to model gas-phase SO_2 oxidation in the atmosphere. The analysis of the v = 1, 2, 3 kinetics in the companion paper indicate a lower value for k_1^{∞}(k_1^{∞}=(7.2 ± 3.3) × 10^{-13} cm^3 molecule^{-1} s^{-1}) than is currently recommended in the literature, ($(2.0^{+2.0}_{-1.0})$ [3] or (1.6 ± 0.4) [4] × 10^{-12} cm^3 molecule^{-1} s^{-1}). To examine k_1 in more detail, the measured rate coefficient for OH(v=0) + SO_2 from this study, together with those from the literature, have been used in a master equation analysis to determine the most consistent values for the system, which should, in turn, be consistent with the vibrationally excited state data reported in the companion paper.

Using the in-built Marquardt algorithm in MESMER, data fitting to the present dataset and the literature has been performed, where the adjustable parameters are A, n (E_a = 0) and the collisional energy transfer parameter, $\langle\Delta E_{down}\rangle$. MESMER can fit to

multiple gases, with differing values of $<\Delta E_{down}>$ so that kinetic data with different buffer gases (helium, argon, nitrogen and SF_6) have been simultaneously fitted. Figure 5 shows a master equation simulation for helium using the parameters from the fit to the $k_1[M]$ data in Figure 7, the most reliable data, see below. This simulation indicates the experimental data are within a factor of two of each other, except for the high pressure values from Fulle et al.,[10] and the low-pressure flow tube data. From this analysis alone it is evident that the low-pressure flow tube data and the high-pressure flash photolysis data are incompatible with the master equation model of $k_1[M]$. Various subsets of kinetic data have been analysed using MESMER in order to check for consistency and to quantify the discrepancy between the data subsets. In the SI the MESMER input file, which contains all the kinetic data considered in this analysis, is provided.

The high-pressure flash photolysis experiments can, potentially, result in photolysis of SO_2 to form radicals – see above – which are reactive towards OH and hence enhance the measured rate coefficients. The low-pressure flow tube experiments do not have any SO_2 photolysis problems, but do generate OH from titration reactions, either H + NO_2/O_3, so that there is the possibility that NO_2 / O_3 can re-generate OH, which leads to lower rate coefficients.

To examine potential problems with the higher pressure (5 – 700 Torr) flash photolysis data, the literature and the present results were analysed and a plot of the measured and calculated k_1 is shown in Figure 6. From this figure it is evident that the fit to the data is scattered (a good example of such analysis, where from many studies the slope is close to 1.0, i.e. good agreement between measured and calculated, can be

found in reference 30), especially the SF_6 data from Wine et al.[8] that indicate the measured rate coefficients are significantly larger than the calculated. In this calculation A, n and $<\Delta E>_{down}$ were floated freely, where each buffer gas had its own independent $<\Delta E>_{down}$. The result from this fitting indicates that over this pressure range k_1^{∞} is defined but fits for each buffer gas lead to different values for k_1^{∞}, hence the different slopes for each gas in Figure 6. If k_1^{∞} were not defined then $<\Delta E>_{down}$ for each gas could be adjusted to obtain a near perfect fit, but k_1^{∞} is defined and no better fit to the data in Figure 6 is possible.

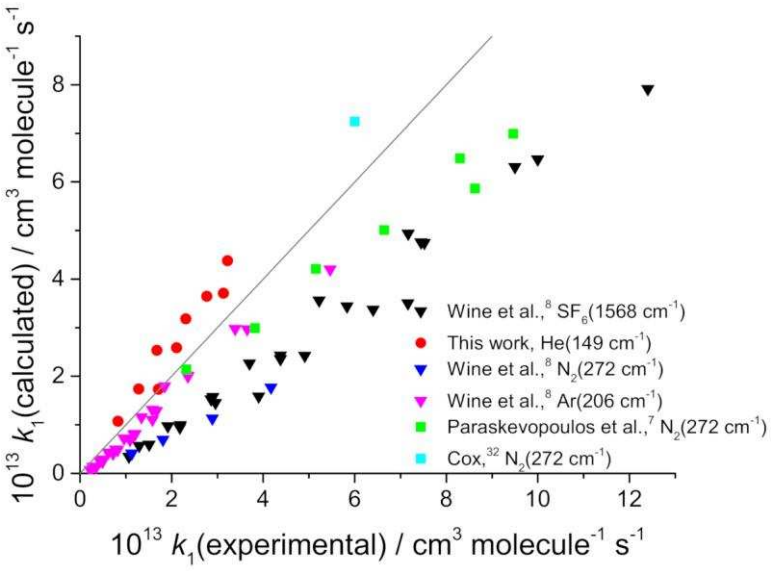

Figure 6. A plot of k_1(calculated) from the master equation analysis of flash photolysis data versus k_1(experimental). It can be seen that the literature k_1 experimental data are generally higher than the calculated value, i.e. below the line with a slope equal to one. The fitted energy transfer parameters, $<\Delta E>_{down}$, are given in brackets after the bath gas.

Removal of the SF_6, N_2 and He data from Wine et al.[8] together with the data from Paraskevopoulos et al. [7] yields a good fit as evidenced in Figure 7. The reason why the SF_6 data from Wine et al.[8] returns k_1 that are significantly larger might be related to the

fact that SF_6 has small, but significant, absorption cross-sections in the VUV region [30] where H_2O was photolysed to produce OH, which leads to additional OH chemistry. However, the reason why only the Ar data from Wine et al.[8] can be fitted well is unclear. Also included in Figure 7 are the data from Cox, [31] where k_1 was determined from the continuous lamp photolysis of HNO_2 in the presence of SO_2. The low intensity of the lamp ensures that there is no SO_2 photolysis in the system, which is not the case in all the laser flash photolysis experiments. The fit to the data in Figure 7 returned k_1^{∞} (295 K) = (7.8 ± 2.2) × 10^{-13} cm^3 $molecule^{-1}$ s^{-1}, where the temperature dependence was fixed and equal to $(T/298)^{0.1}$; this value of n is from our OH/OD(v=1,2,3)+SO_2 data, see the companion paper, and is required as most of the temperature-dependent data have been removed from the analysis. This is our best determination of k_1^{∞}.

The OD + SO_2 data, see Figure 5 and Table 2, were also fitted using MESMER. The input parameters are similar to OH + SO_2 except for three vibrations and the zero point energy adjustment of the well-depth; input parameters are given in the SI. An excellent fit was obtained, similar to Figure 7, and yielded the parameters: $k_{1,D}^{\infty}$(295 K) = (8.7 ± 2.6) × 10^{-13} cm^3 $molecule^{-1}$ s^{-1} and $\langle\Delta E\rangle_{down}$ = 197 ± 48 cm^{-1}. As the kinetic isotope in reaction R1 is reasonably expected to be close to zero, $k_{1,D}^{\infty}$ and k_1^{∞} should be the same. Within error, this is the case and hence provides further evidence of our assignment of k_1^{∞}.

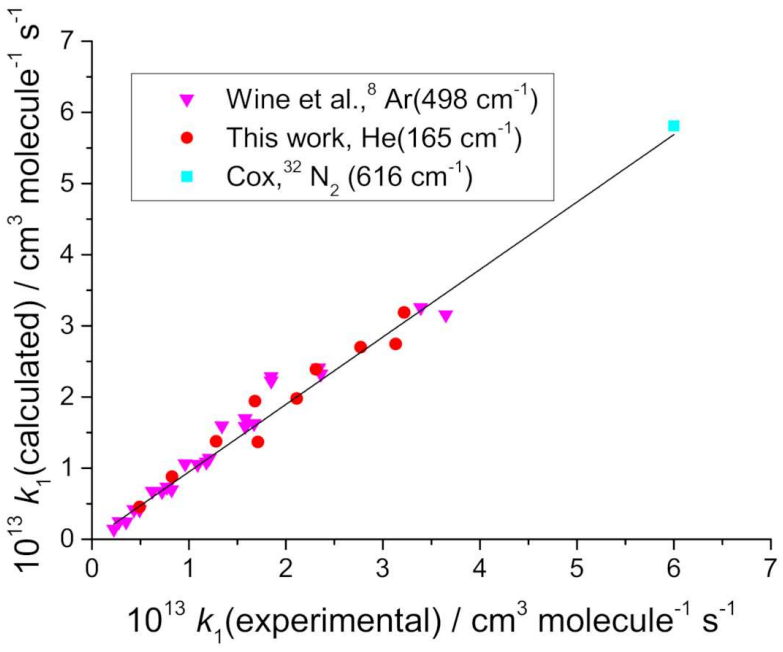

Figure 7. A plot of k_1(calculated) versus k_1(experimental) from the MESMER fit to selected flash photolysis data, see text. The slope is equal to 0.97 and the returned value k_1^{∞}(295 K) = (7.8 ± 2.2) × 10^{-13} cm^3 $molecule^{-1}$ s^{-1}, 2σ. The fitted energy transfer parameters, $\langle\Delta E\rangle_{down}$, are given in brackets after the bath gas.

The low-pressure flow tube data have been examined by combining our dataset from Figure 7, with the flow tube data (helium bath gas) from Leu and Lee et al.[5, 26] and fitted by MESMER, where k_1^{∞} was fixed to (7.8 ± 2.2) × 10^{-13} cm^3 $molecule^{-1}$ s^{-1} and the helium energy transfer parameter is also fixed, $\langle\Delta E_{down}\rangle$ = 165 cm^{-1}.

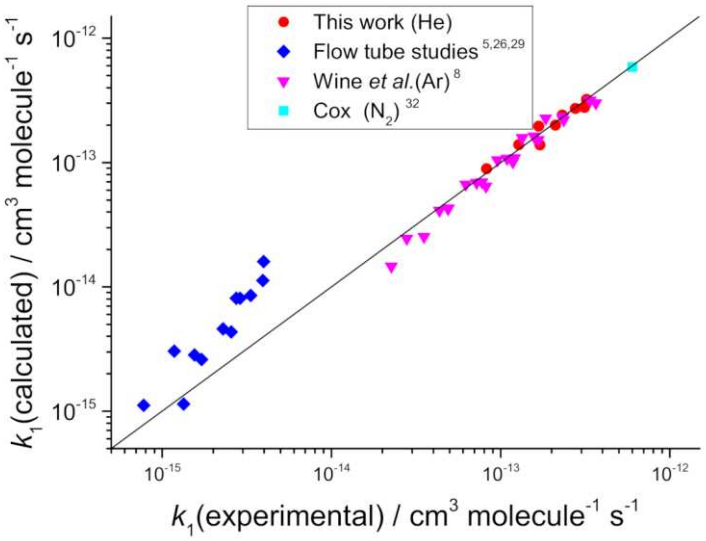

Figure 8. A log-log plot of k_1(calculated) versus k_1(experimental) from the MESMER analysis of the data in Figure 7 and the flow tube data from [5, 26, 29] where helium is the buffer gas and its $\langle\Delta E\rangle_{down}$ parameter is fixed to 165 cm^{-1}. The black line is a slope of 1.0.

The quality of the fit is seen in Figure 8 via a log-log plot, where it can be seen that the low pressure data are poorly fitted with experimental values up to a factor of 3 below the calculated values. A possible explanation of this observation is that the products of the reaction recycle back to OH and hence lower the observed k_1. Some evidence to support this explanation is the observation by Lee et al.[5] of a factor two lower rate coefficient when O_2 was the buffer gas compared to nitrogen. In general, the buffer gas efficiency of O_2 and N_2 are similar. In the study by Leu, [26] attempts to observe products, $HOSO_2$, SO_3 and H_2SO_4, via mass spectrometry were unsuccessful, and it was suggested that *"these molecules may condense and/or react with* H_2O on the surface of the flow tube.*"*

Overall, it is concluded that the data shown in Figure 7 yield the best kinetic parameters on the OH + SO_2 reaction and $k_1^{\infty}(295\ K) = (7.8 \pm 2.2) \times 10^{-13}$ cm^3 $molecule^{-1}$ s^{-1}. In general, k_1 from the flash photolysis studies are too large because SO_2 photolysis

has not been taken into account and the flow tube data yields k_1 that are too small, possibly arising from OH recycling. Therefore only a limited dataset has been used to determine $k_1(p,T)$. $k_1^{\infty}(295\ K)$ is reasonably determined but its temperature dependence is much more uncertain. Hence the temperature dependence has been fixed to $(T/298)^{0.1}$, determined from our OH(v=1,2,3)+SO_2 data, which was studied between 295 – 810 K, see companion paper. The current IUPAC and JPL recommended values for k_1^{∞} are $(2.0^{+2.0}_{-1.0})$ and $(1.6 \pm 0.4) \times 10^{-12}$ cm^3 $molecule^{-1}$ s^{-1}, which are over a factor two larger than the current determination. But this recommendation is influenced by data that are affected by SO_2 photolysis, see above, and our previous rate coefficient determination for OH(v=1)+SO_2, which was assumed to be a proxy for k_1^{∞} but is actually an overestimation as it did not account for direct energy transfer, see the companion paper.

Using our optimum parameterisation of $k_1^{\infty}(T)$ of $(7.8 \pm 2.2) \times 10^{-13}$ $(T/298)^{0.1}$ cm^3 $molecule^{-1}$ s^{-1}, MESMER has been used to generate a dataset that has been parameterised using a Troe formalism,[32] using the same representation in a previous paper on CH_3O_2 + NO_2.[32] This dataset has been produced using an estimated energy transfer parameter for nitrogen (N_2 and O_2 are usually similar) equal to $\langle\Delta E_{down}\rangle(N_2)/cm^{-1} = 600 \times (T/298)^{0.3}$; the value from data fitting to Figure 7 is based only on one nitrogen data point from Cox, so has a very large error bar. These MESMER simulations have been carried out over the temperature range 200 – 600 K and Table 3 gives the derived Troe parameters for nitrogen. The results are shown in Figure 9.

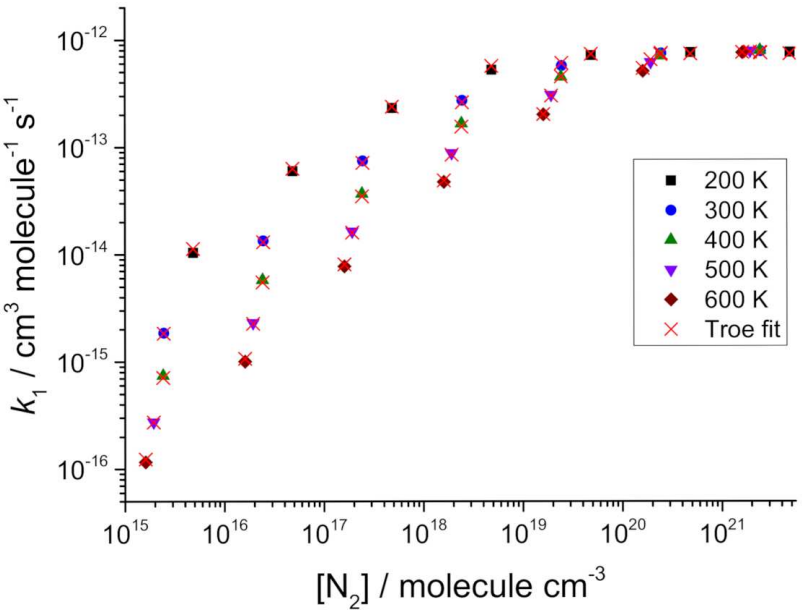

Figure 9. Troe fit (cross) to the dataset (symbols) generated from the MESMER simulation of $k_1^{\infty}(T) = (7.8 \pm 2.2) \times 10^{-13} (T/298)^{0.1}$ cm^3 molecule^{-1} s^{-1} and $\langle\Delta E_{down}\rangle(N_2) / cm^{-1} = 600 \times (T/298)^{0.3}$ over the temperature and pressure range 200 – 600 K and 10^{15} - 10^{22} molecule cm^{-3}.

From Figure 9 it can be seen that these Troe fits are an adequate description of the master equation output. Currently, the IUPAC [3] and JPL [4] recommended rate coefficient at 298 K and 1 bar N_2 are 8.9 and 9.5×10^{-13} cm^3 molecule^{-1} s^{-1} , respectively, while the present study recommends a rate coefficient of 5.8×10^{-13} cm^3 molecule^{-1} s^{-1}. This difference translates itself in both the low and high-pressure limiting rate coefficients: $k_1^{\infty} = 7.8 \times 10^{-13}$ cm^3 molecule^{-1} s^{-1} (present) versus $k_1^{\infty} = 2.0$ and 1.6×10^{-12} cm^3 molecule^{-1} s^{-1} (IUPAC and JPL); $k_1^0(N_2,T) = 1.10 \times 10^{-30} \times (T/298)^{-3.62}$ cm^6 molecule^{-2} s^{-1} (present) versus $k_1^0(N_2,T) = 2.5 \times (T/300)^{-2.6}$ and $3.3 \times 10^{-31} \times (T/298)^{-4.3}$ cm^6 molecule^{-2} s^{-1} (IUPAC and JPL). Both k_1^{∞} and $k_1^0(N_2)$ from the current study are markedly different to the recommended IUPAC and JPL values. The temperature dependence of $k_1^0(N_2)$ is distinctly negative and while the present value, $(T/300)^{-3.6}$, is

based on a tuned master equation model the IUPAC and JPL values are based on fits to the literature.

6. Conclusions and summary

(i) The rate coefficients for the removal OH(v=0) by SO_2, k_1, has been studied using laser flash photolysis coupled with laser induced fluorescence. It is evident that the 248 nm excimer laser fluences used induced two photon dissociation of SO_2 to $O(^1D)$. The second photon absorption to give $O(^1D)$, σ_2, has been determined ($\sigma_2 = (5.5 \pm 2.0) \times 10^{-18}$ cm^2 $molecule^{-1}$). Other photoproducts from this two photon photolysis contributed to the decay of OH; this interference was minimised by reducing the laser energy as $[SO_2]$ was increased to generate a constant photolysis yield of all species.

(ii) Experiments were carried out where the photolysis energy of the laser was adjusted to keep the amount of SO_2 photolysis constant and hence determine a more accurate value of k_1.

(iii) Master equation analysis using MESMER has been used to fit the current dataset and that from the literature. From this it is apparent that much of the flash photolysis data are contaminated from SO_2 photolysis, and results in k_1 values that are too large. A much reduced dataset was used in the determination k_1^{∞}. This k_1^{∞} value was reinforced from the MESMER analysis of the OD + SO_2 data.

(iv) The master equation model of $k_1(p,T)$ was used to fit to the low pressure flow tube data and a poor fit was observed. At low pressures the experimental data were

much smaller than the predicted. It is speculated that this results from an uncharacterised OH recycling mechanism.

(v) Comparison of k_1 from this study and the currently recommended values from IUPAC and JPL shows poor agreement: our value for k_1^{∞} is over a factor of two smaller and our value for k_1^0 is over a factor of three larger.

(vi) Using parameters from fitting to our refined dataset, the output from a master equation simulation for nitrogen buffer gas has been parameterized using a Troe-formalism to provide an analytical description of k_1 over the range T = 200 – 600 K and $[N_2] = 10^{15} – 10^{21}$ molecule cm^{-3}. At 298 K our current estimate and the recommended values from IUPAC and JPL for k_1(1 Bar N_2) is equal to 5.8 and (8.9 and 9.5) × 10^{-13} cm^3 $molecule^{-1}$ s^{-1}, respectively.

Acknowledgements

We thank Mike Pilling for providing helpful discussions and proof reading this manuscript, and Diogo Medeiros for performing calculations on OD + SO_2. Also, we are grateful to NERC (NE/K005820/1) and EPSRC (GR/T28560/01) for funding.

Supporting Information Available

The supporting information contains the input file for the MESMER master equation analysis.

References

1. Blitz, M. A.; Hughes, K. J.; Pilling, M. J. Determination of the High-Pressure Limiting Rate Coefficient and the Enthalpy of Reaction for OH + SO_2. J. Phys. Chem. A **2003,** 107, 1971-1978.
2. Jaffer, D. H.; Smith, I. W. M. Time-Resolved Measurements on the Relaxation of OH(v = 1) by NO, NO_2 AND O_2. Faraday Disc. **1979,** 67, 212-220.
3. Atkinson, R.; Baulch, D. L.; Cox, R. A.; Crowley, J. N.; Hampson, R. F.; Hynes, R. G.; Jenkin, M. E.; Rossi, M. J.; Troe, J. Evaluated Kinetic and Photochemical Data for Atmospheric Chemistry: Volume I - Gas Phase Reactions of Ox, HOx, NOx and SOx Species. Atmos. Chem. Phys. **2004,** 4, 1461-1738.
4. Burkholder, J. B.; Sander, S. P.; Abbatt, J.; Barker, J. R.; Huie, R. E.; Kolb, C. E.; Kurylo, M. J.; Orkin, V. L.; Wilmouth, D. M.; Wine, P. H. "Chemical Kinetics and Photochemical Data for Use in Atmospheric Studies, Evaluation No. 18," JPL Publication 15-10, Jet Propulsion Laboratory, Pasadena. 2015 http://jpldataeval.jpl.nasa.gov.
5. Lee, Y. Y.; Kao, W. C.; Lee, Y. P. Kinetics of the Reaction Hydroxyl + Sulfur Dioxide in Helium, Nitrogen, and Oxygen at Low Pressure. J. Phys. Chem. **1990,** 94, 4535-4540.
6. Martin, D.; Jourdain, J. L.; Laverdet, G.; Le Bras, G. Kinetic Studies of Oxidation Reactions of Sulfur Compounds: Reaction Sulfur Dioxide + Hydroxyl in the presence of Oxygen and Reaction Iodine Oxide (IO) + DMS; CNRS: 1987; pp 212-217.
7. Paraskevopoulos, G.; Singleton, D. L.; Irwin, R. S. Rates of Hydroxyl Radical Reactions. The Reaction Hydroxyl Radical + Sulfur Dioxide + Molecular Nitrogen. Chem. Phys. Lett. **1983,** 100, 83-87.
8. Wine, P. H.; Thompson, R. J.; Ravishankara, A. R.; Semmes, D. H.; Gump, C. A.; Torabi, A.; Nicovich, J. M. Kinetics of the Reaction OH + SO_2 + M → $HOSO_2$ + M. Temperature and Pressure Dependence in the Fall-Off Region. J. Phys. Chem. **1984,** 88, 2095-2104.
9. Cobos, C. J.; Troe, J. Theory of Thermal Unimolecular Reactions at High Pressures. II. Analysis of Experimental Results. J. Chem. Phys. **1985,** 83, 1010-1015.
10. Fulle, D.; Hamann, H. F.; Hippler, H. The Pressure and Temperature Dependence of the Recombination Reaction HO + SO_2 + M → $HOSO_2$ + M. Phys. Chem. Chem. Phys. **1999,** 1, 2695-2702.
11. Glowacki, D. R.; Liang, C.-H.; Morley, C.; Pilling, M. J.; Robertson, S. H. MESMER: An Open-Source Master Equation Solver for Multi-Energy Well Reactions. J. Phys. Chem. A **2012,** 116, 9545-9560.
12. McKee, K. W.; Blitz, M. A.; Cleary, P. A.; Glowacki, D. R.; Pilling, M. J.; Seakins, P. W.; Wang, L. Experimental and Master Equation Study of the Kinetics of OH + C_2H_2: Temperature Dependence of the Limiting High Pressure and Pressure Dependent Rate Coefficients. J. Phys. Chem. A **2007,** 111, 4043-4055.
13. Klopper, W.; Tew, D. P.; Gonzalez-Garcia, N.; Olzmann, M. Heat of Formation of the $HOSO_2$ Radical from Accurate Quantum Chemical Calculations. J. Chem. Phys. **2008,** 129, 114308/1-114308/7.
14. Barker, J. R. Multiple-Well, Multiple-Path Unimolecular Reaction Systems. I. MultiWell Computer Program Suite. Int. J. Chem. Kinet. **2001,** 33, 232-245.
15. Klippenstein, S. J.; Miller, J. A. From the Time-Dependent, Multiple-Well Master Equation to Phenomenological Rate Coefficients. J. Phys. Chem. A **2002,** 106, 9267-9277.

16. Miller, J. A.; Klippenstein, S. J. Master Equation Methods in Gas Phase Chemical Kinetics. J. Phys. Chem. A **2006,** 110, 10528-10544.
17. Pilling, M. J.; Robertson, S. H. Master Equation Models for Chemical Reactions of Importance in Combustion. Annu. Rev. Phys. Chem. **2003,** 54, 245-275.
18. Davies, J. W.; Green, N. J. B.; Pilling, M. J. The Testing of Models for Unimolecular Decomposition via Inverse Laplace Transformation of Experimental Recombination Rate Data. Chem. Phys. Lett. **1986,** 126, 373-379.
19. Kenneth A. Holbrook; Michael J. Pilling; Robertson, S. H. Unimolecular Reactions, 2nd Edition. John Wiley & Sons: New York, 1996; p 434
20. Blitz, M. A.; Green, N. J. B.; Shannon, R. J.; Pilling, M. J.; Seakins, P. W.; Western, C. M.; Robertson, S. H. Reanalysis of Rate Data for the Reaction $CH_3 + CH_3 \rightarrow C_2H_6$ Using Revised Cross Sections and a Linearized Second-Order Master Equation. J. Phys. Chem. A **2015,** 119, 7668-7682.
21. Effenhauser, C. S.; Felder, P.; Huber, J. R. 2-Photon Dissociation of Sulfur-Dioxide at 248 nm and 308 nm. Chem. Phys. **1990,** 142, 311-320.
22. Aker, P. M.; Sloan, J. J. The Initial Product Vibrational-Energy Distribution in the Reaction between $O(^1D)$ and H_2. J. Chem. Phys. **1986,** 85, 1412-1417.
23. Kovacs, T.; Blitz, M. A.; Seakins, P. W.; Pilling, M. J. H atom Formation from Benzene and Toluene Photoexcitation at 248 nm. J. Chem. Phys. **2009,** 131, 204304/1-204304/12.
24. Hermans, C.; Vandaele, A. C.; Fally, S. Fourier Transform Measurements of SO_2 Absorption Cross Sections. J. Quant. Spectrosc. Radiat. Transfer **2009,** 110, 756-765.
25. Baasandorj, M.; Papanastasiou, D. K.; Talukdar, R. K.; Hasson, A. S.; Burkholder, J. B. $(CH_3)_3COOH$ (tert-Butyl Hydroperoxide): OH Reaction Rate Coefficients between 206 and 375 K and the OH Photolysis Quantum Yield at 248 nm. Phys. Chem. Chem. Phys. **2010,** 12, 12101-12111.
26. Leu, M. T. Rate Constants for the Reaction of Hydroxyl with Sulfur Dioxide at Low Pressure. J. Phys. Chem. **1982,** 86, 4558-62.
27. Castleman, A. W., Jr.; Tang, I. N. Kinetics of the Association Reaction of Sulfur Dioxide with the Hydroxyl Radical. J. Photochem. **1977,** 6, 349-354.
28. Harris, G. W.; Wayne, R. P. Reaction of Hydroxyl Radicals with Nitric Oxide, Nitrogen Dioxide, and Sulfur Dioxide. J. Chem. Soc., Faraday Trans. 1 **1975,** 71, 610-617.
29. Martin, D.; Jourdain, J. L.; G., L. B. Discharge Flow Measurements of the Rate Constants for the Reaction $OH + SO_2 + He$ and $HOSO_2 + O_2$ in Relation with the Atmospheric Oxidation of Sulfur Dioxide. J. Phys. Chem. **1986,** 90, 4143-4147.
30. Pradayrol, C.; Casanovas, A. M.; Deharo, I.; Guelfucci, J. P.; Casanovas, J. Absorption Coefficients of SF_6, SF_4, SOF_2 and SO_2F_2 in the Vacuum Ultraviolet. J. De Physique Iii **1996,** 6, 603-612.
31. Cox, R. A. Photolysis of Gaseous Nitrous Acid. Technique for Obtaining Kinetic Data on Atmospheric Photooxidation Reactions. Int. J. Chem. Kinet. **1975,** 7, 379-398.
32. McKee, K.; Blitz, M. A.; Pilling, M. J. Temperature and Pressure Studies of the Reactions of CH_3O_2, HO_2, and 1,2-$C_4H_9O_2$ with NO_2. J. Phys. Chem. A **2016,** 120, 1408-1420.
33. Troe, J.; Ushakov, V. G. Representation of "Broad" Falloff Curves for Dissociation and Recombination Reactions. Z. Phys. Chem. (Muenchen, Ger.) **2014,** 228, 1-10.

Table 1. Rate coefficients for OH ($\nu = 0$) + SO_2 at various pressures in He. The uncertainties are 1σ standard deviations.

T / K	[He] / Torr	10^{13} k_1 / (cm^3 $molecule^{-1}$ s^{-1})
295	24.9	0.83 ± 0.08
295	52.2	1.71 ± 0.17
295	52.5	1.28 ± 0.13
295	100.3	1.68 ± 0.17
295	104	2.11 ± 0.23
295	154	2.31 ± 0.21
295	202.2	2.77 ± 0.28
295	209.9	3.13 ± 0.31
295	301.2	3.22 ± 0.63

Table 2. Rate coefficients for OD ($\nu = 0$) + SO_2 at various pressures in He. The uncertainties are 1σ standard deviations.

T / K	[He] / Torr	10^{13} k_1 / (cm^3 $molecule^{-1}$ s^{-1})
295	27.7	1.17 ± 0.12
295	49.7	1.80 ± 0.18
295	103.1	2.36 ± 0.24
295	154.9	3.13 ± 0.31
295	200.3	3.15 ± 0.32
295	303.4	4.07 ± 0.41

Table 3.

Table 3. OH + SO_2 Troe parameters [33] for nitrogen buffer gas.

$k_1(p,T)$:
$k^{\infty}(T) = 7.55\times10^{-13} \times (T/298)^{0.041}$ cm^3 $molecule^{-1}$ s^{-1}
$k_0(T) = 1.10\times10^{-30} \times (T/298)^{-3.62}$ cm^6 $molecule^{-2}$ s^{-1}
$x_0 = 0.30$
b = 1.30
$F_{cent} = 0.125 \times \exp(0.000221 \times T)$

Figure Captions

Figure 1. OH production from P1 and R2 as a function of excimer laser intensity. The duration of the excimer laser pulse was 20 ns. The red line is a quadratic function fitted to the data.

Figure 2. OH(v=0) + SO_2 (2.35×10^{16} molecule cm^{-3}) at 50 Torr total pressure, helium. t-$(CH_3)_3COOH$ was used to generate ground-state hydroxyl radical. Analysis of these data (E8) yields $k_{obs} = (3643 \pm 63)$ s^{-1}, where the error is statistical at the 1 σ level. The red line is the best fit to the data.

Figure 3. OD(v=0) from the photolysis of SO_2 (6.05×10^{15} cm^{-3}) / D_2 at a total pressure of 100 Torr, helium buffer. At early times there is growth due to relaxation from higher vibrational states, OD(v>0). Soon after the maximum in the OD signal the decay is described by a single exponential (blue curve), which via Eqn (E8) gives $k_{obs} = 2107 \pm 60$ s^{-1}. The red line is a biexponential fit to the data and yields $k_{obs} = 2232 \pm 69$ s^{-1}.

Figure 4 Bimolecular plot of k_{obs} vs [SO_2] for OH(v=0) + SO_2 at 50 Torr total pressure, helium buffer; $k_1 = (1.28 \pm 0.03) \times 10^{-13}$ cm^3 $molecule^{-1}$ s^{-1}.

Figure 5. Literature rate coefficients, k_1, for the reaction OH + SO_2, at room temperature, where helium is the bath gas. Our results for OD + SO_2 are also included. The solid line is a master equation simulation for OH + SO_2 using helium and the parameters from the fit to the k_1[M] data in Figure 7, the most reliable data set, see text for details.

Figure 6. A plot of k_1(calculated) from the master equation analysis of flash photolysis data versus k_1(experimental). It can be seen that the literature k_1 experimental data are generally lower than the calculated value, i.e. below the line with a slope equal to one. The fitted energy transfer parameters, $\langle\Delta E\rangle_{down}$, are given in brackets after the bath gas.

Figure 7. A plot of k_1(calculated) versus k_1(experimental) from the MESMER fit to selected flash photolysis data, see text. The slope is equal to 0.97 and the returned value $k_1^{\infty}(295\ K) = (7.8 \pm 2.2) \times 10^{-13}$ cm^3 $molecule^{-1}$ s^{-1}, 2σ. The fitted energy transfer parameters, $\langle\Delta E\rangle_{down}$, are given in brackets after the bath gas.

Figure 8. A log-log plot of k_1(calculated) versus k_1(experimental) from the MESMER analysis of the data in Figure 7 and the flow tube data from [5, 26, 29] where helium is the buffer gas and its $<\Delta E>_{down}$ parameter is fixed to 165 cm^{-1}. The black line is a slope of 1.0.

Figure 9. Troe fit(cross) to the dataset(symbols) generated from the MESMER simulation of $k_1^{\infty}(T) = 7.8 \pm 2.2 \times 10^{-13} (T/298)^{0.1}$ cm^3 $molecule^{-1}$ s^{-1} and $<\Delta E_{down}>(N_2) / cm^{-1} = 600 \times (T/298)^{0.3}$ over the temperature and pressure range 200 – 600 K and 10^{15} - 10^{22} molecule cm^{-3}.

TOC Graphic

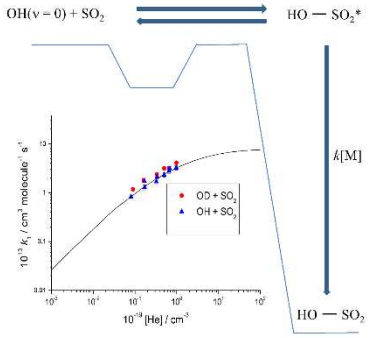
OH(v = 0) + SO2
HO — SO2*
k[M]
HO — SO2
OD + SO2
OH + SO2
10^-13 k1 / cm^3 molecule^-1 s^-1
10^-19 [He] / cm^-3